Indian J Otolaryngol Head Neck Surg
(November 2019) 71(Suppl 3):S2231–S2240; https://doi.org/10.1007/s12070-019-01716-9

ORIGINAL ARTICLE

Anatomical Variations of the Nose and Paranasal Sinuses: A Computed Tomographic Study

K. Devaraja[1] · Shreyanka M. Doreswamy[1] · Kailesh Pujary[1] · Balakrishnan Ramaswamy[1] · Suresh Pillai[1]

Received: 31 May 2019 / Accepted: 11 July 2019 / Published online: 26 July 2019

Abstract To evaluate the anatomical variations in computed tomographic (CT) images of paranasal sinuses and to investigate association between them. Design: Retrospective study. Setting: Tertiary care center in the southern part of India. Subjects: Radiological images of paranasal sinuses belonging to chronic rhinosinusitis patients managed between June 2016 and November 2018. Methods: The studied characteristics in the CT images included the deviated nasal septum (DNS), concha bullosa (CB), Haller cell (HC), Onodi cell (OC), pneumatization of anterior clinoid process (ACP), pterygoid base (PB), superior turbinate, inferior turbinate, crista galli (CG), and nasal septum. The height of the lateral lamella of the cribriform plate, the sphenoid pneumatization pattern, and the optic nerve relationship with sphenoid sinus were studied separately. The associations between these factors, and with maxillary sinus opacifications were also investigated. A total of 151 adult patients' CT images were analyzed. The most common manifestations noted were DNS, CB and pneumatized PB, seen in 83.4%, 49% and 47% of the patients respectively. The rates of HC, OC, pneumatized septum, pneumatized CG, and pneumatized ACP were 39%, 23%, 27%, 43% and 27% in that order. Rates of most of these variations were within the range reported in the literature. Chi square test revealed that the OC was independently associated with pneumatized CG and pneumatized septum. The maxillary sinus opacification was related to DNS and CB, but not with protrusion of tooth root into the sinus. Most of the anatomical variations were comparable with the reports across the globe, however, the associations between these variations weren't common in our cohort.

Keywords Anatomical variations · Computed tomography · Paranasal sinuses · Sphenoid sinus · Concha bullosa · Pneumatization

Introduction

Anatomical characteristics of the nose and paranasal sinuses exhibit considerable variations. Many of those perturbations vary depending on age, gender, geography, race, and ethnicity, though some differences aren't significant statistically [1–8]. Nevertheless, quite a few of these variations have been linked to aetiopathogenesis of inflammatory sinonasal diseases [9–12]. Knowledge about these variations is not only relevant diagnostically, but also play a significant role in reducing the intraoperative difficulties and post-operative complications of endoscopic or open sinus surgery/skull base surgery [5, 13–17]. Computed tomography (CT) of the nose and paranasal sinus is of paramount importance in detecting the type and extent of anatomical perturbations in this region. Though the prevalence rates and patterns of the variations have been studied radiologically in the past, studies looking into almost all of the anatomical differences comprehensively in the same cohort are very sparse. Most of the existing studies, including those from this region are of lesser sample size and have evaluated limited parameters [7, 18–21]. The present study with larger sample size describes almost all the anatomical variations of paranasal sinuses in the study cohort. Furthermore, the study

✉ Suresh Pillai
surpil21@gmail.com

1 Department of Otorhinolaryngology and Head and Neck Surgery, Kasturba Medical College, Manipal, Manipal Academy of Higher Education, Udupi, Karnataka 576104, India

uniquely explores some of the clinico-radiological parameters like tooth root location in the maxillary sinus, the maxillary septation, the unsafe nature of the sphenoid septation, most of which have not been defined in the previous studies.

The primary objective of this study was to evaluate the anatomical variations in CT images of the nose and paranasal sinuses in a cohort of patients having inflammatory sinonasal diseases, in the form of chronic rhinosinusitis. Subset analysis in the study was meant to investigate associations between the various anatomical perturbations if any. And lastly, the study also tries to establish the clinically meaningful correlations between the prominent anatomical variations and corresponding clinical manifestations of sinonasal diseases.

Materials and Methods

It is a retrospective study done at a tertiary care medical center in the southern part of India. After obtaining the institute's ethical committee approval, the CT images of the nose and paranasal sinuses of chronic rhinosinusitis patients managed by the Department of Otorhinolaryngology between June 2016 and November 2018 were retrieved for the analysis in this study. The CT on these patients was done using 64 slice Philips Brilliance, Philips Healthcare Suzhou Co Ltd, China. The 3 mm axial images were acquired cranio-caudally from the highest point of frontal sinus to the lowest part of the maxillary sinus and then reconstructed to 0.6 mm slices multiplanar images. The anatomical variations and their characteristics noted in the CT images included the deviated nasal septum (DNS), the concha bullosa (CB), the Haller cell (HC), the Onodi cell (OC), pneumatization of the anterior clinoid process (ACP), the pterygoid base (PB), the superior turbinate (ST), the inferior turbinate (IT), the crista galli (CG) and the nasal septum. Apart from the prevalence rates of these variations, the classifications, and the laterality were studied, and the relevant associations were investigated. DNS was classified radiologically into obstructive or simple, depending on whether or not the septum is touching the lateral wall or the turbinate on the ipsilateral side. The CB was classified as bullous, lamellar or extensive based on which part of the middle turbinate [MT] is pneumatized, whether bulla, lamella, or both. The variations in the depth of olfactory fossa, the relationship of the optic nerve to sphenoid sinus wall and the sphenoid pneumatization were analyzed separately.

The olfactory fossa depth was represented by the height of the lateral lamella of the cribriform plate and was classified into three types as per the Keros' classification system [22]. Similarly, the relationship of the optic nerve to the sphenoid sinus wall was categorized as per Delano et al. [21, 23]. The sphenoid pneumatization itself was classified into either of conchal, pre-sellar, sellar and post-sellar varieties depending on the extent of exposure of sella turcica into the sphenoid sinus [3, 7, 24–27]. The study also explores the prevalence of the unsafe type of sphenoid septation that is having an attachment to the intra-cavernous carotid artery or optic nerve, and the implications of protrusion of tooth root into the maxillary sinus in its opacification. Accordingly, to verify the association of maxillary sinus opacification with tooth root, DNS, CB or HC, the maxillary sinuses and these characteristics were considered separately on each side, except for DNS, for which the presence of maxillary opacification on either of side was deemed to be positive.

The first two authors together evaluated the coronal, the sagittal, and the axial images of all the patients and assigned each anatomical characteristic an agreed type or grade or both, wherever applicable. In case of any disagreements or ambiguity in any parameter, the report given by the radiologist was taken into consideration, and the said features were assigned accordingly. CT images of those patients who were of age less than 18 years and those who had undergone surgery in the past were excluded from the study. The demographic data, the clinical manifestations, and the radiological characteristics were tabulated separately into a spreadsheet. Using the STATA 13.1 (StataCorp. 2013, College Station, TX: StataCorp LP), the appropriate statistical tests were performed to find out clinically relevant associations between these variables.

Results

The included patients were either partial responders or non-responders to maximal medical therapy for chronic rhinosinusitis and were managed by surgical intervention encompassing balloon sinoplasty, middle meatal antrostomy, frontoethmoidectomy or functional endoscopic sinus surgery, depending on the extent of the disease. These patients had been subjected to plain CT of the nose and paranasal sinuses before their operation, which was retrieved from the digital repository of the institute and was analyzed in this study. A total of 151 patients' CT images have been analyzed in this study. All the patients included were adults aged between 18 and 71 years, with a mean age of 42 years. The majority were male patients [n = 101] with a male: female ratio of 2:1. The anatomical variations and their types/grades noted in the CT images of the study cohort have been summarized in Table 1. Representative CT images of the anatomical differences identified in this study are shown in Figs. 1, 2, 3 and 4. The most common anatomical variation identified was deviated nasal septum

Table 1 Summary of anatomical variations seen in the present study

Anatomical variation	Prevalence and characteristics of the variation (type/grade) (in brackets = number of patients)
Deviated nasal septum	83.4% (126); Simple—79, Obstructive—47
	Symptomatic—85.7% (108 of 126)
Concha bullosa	49% (74) (33 patients had bilateral); *Total CB = 107/302*
	Extensive—43, Lamellar—36, Bullous—28
Haller cell	39% (59) (42 patients had bilateral); *Total HC = 101/302*
Onodi cell	23.1% (35) (24 bilateral); *Total OC = 59/302*
Maxillary sinus septation	5.9% (9) (only 1 bilateral); *Total = 10/302*
Unsafe sphenoid septation	24% (37) (9 bilateral); *Total = 46/302*
Carotid exposed	0.1% (2) (1 bilateral); *Total = 3/302*
Extra pneumatization	Superior turbinate—3.9% (6) (1 bilateral); *Total = 7/302*
	Inferior turbinate—0.6% (only 1, Unilateral); *Total = 1/302*
	Septum—27.1% (41)
	Crista galli– 43% (65)
	Anterior clinoid process—27.1% (41) (26 bilateral); *Total = 67/302*
	Pterygoid base—47% (71) (39 bilateral); *Total = 110/302*
Sphenoid pneumatization	Conchal- 5, Presellar-14, Sellar-49, Post sellar-83 (n = 151)
Olfactory fossa depth	Kero; I—10, II—134, III—7 (n = 151)
Optic nerve relationship	DeLano; 1-61, II-129, III-68, IV-44,(*n = 302*) (13 patients had asymmetrical, 8 of which had type 4 on one side)

Note that the prevalence rates are calculated for the total number of patients, whereas the overall numbers [*in Italics*] given in the corresponding row are calculated considering both the sides of paranasal sinuses separately, wherever relevant

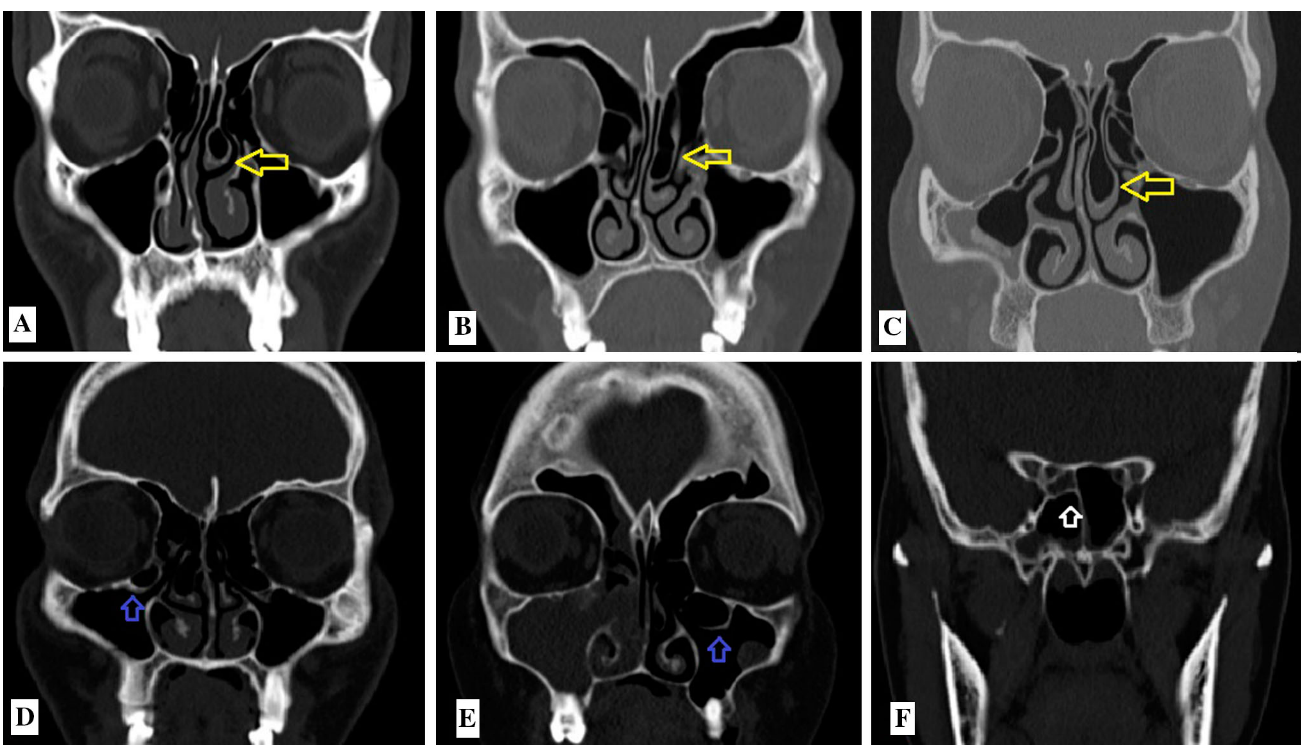

Fig. 1 Coronal images of plain computer tomography of paranasal sinus showing, **a** bulbous type, **b** lamellar type and **c** extensive type of concha bullosa [yellow arrows], **d**, **e** haller cell [blue arrows], **f** onodi cell [white arrow]

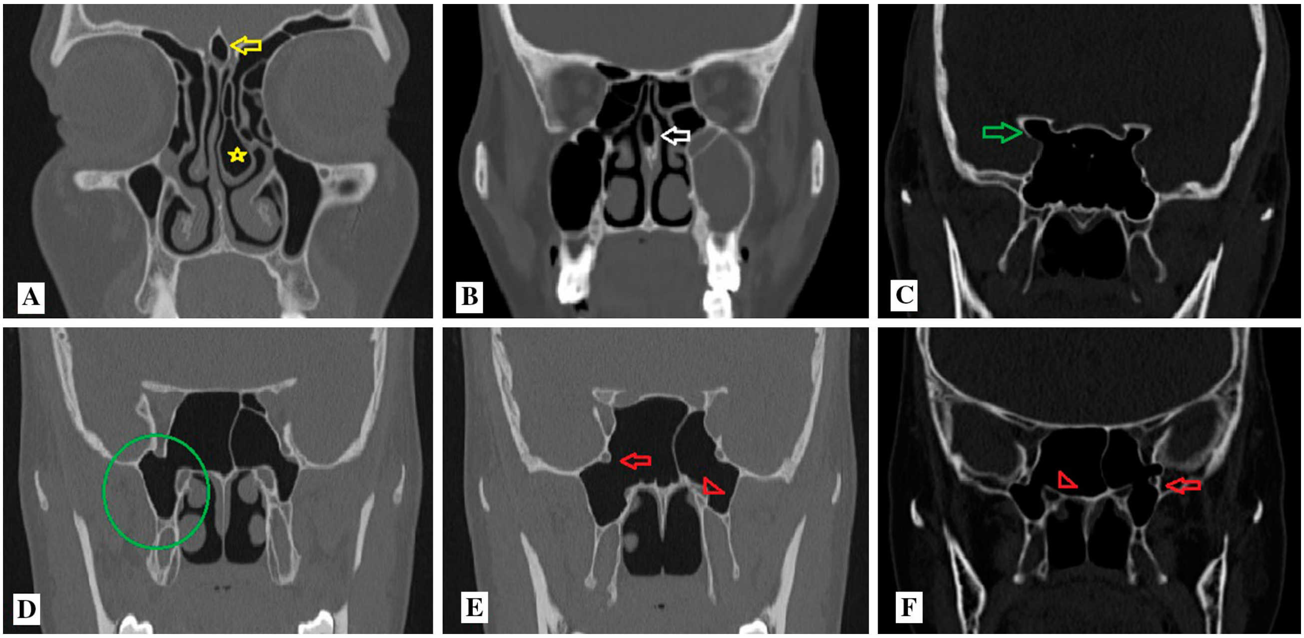

Fig. 2 Coronal images of plain computer tomography of paranasal sinus showing, **a** pneumatized crista galli [yellow arrow] and extensive type of concha bullosa [asterisk], **b** pneumatized nasal septum [white arrow], **c** pneumatized anterior clinoid process [green arrow], **d**–**f** pneumatized pterygoid base [green circle], exposed maxillary nerve [red arrows] and exposed vidian nerve [red arrowheads]

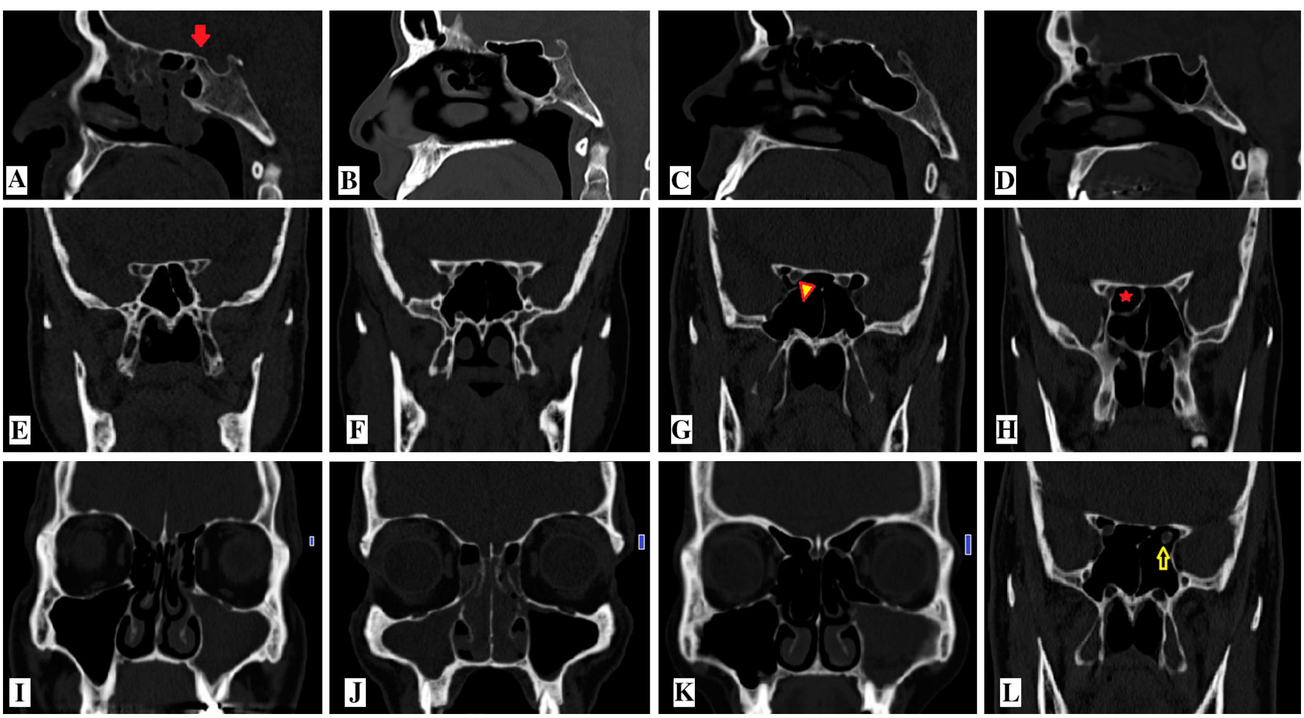

Fig. 3 Plain tomography of paranasal sinuses, first row of sagittal images showing sphenoid pneumatization pattern, **a** conchal type, **b** pre-sellar, **c** sellar and **d** post-sellar; second row of coronal images showing optic nerve relationship with sphenoid sinus wall as per Delano et al. classification, **e** Type I, **f** Type II, **g** Type III [triangle pointing the exposed optic nerve], **h** Type IV [star inside Onodi cell]; third row consisting of coronal images representing the depth of olfactory fossa as per Keros classification, **i** Keros I, **j** Keros II and **k** Keros III [blue line representing the depth], **l** Type III Delano with exposed optic nerve [yellow arrow]

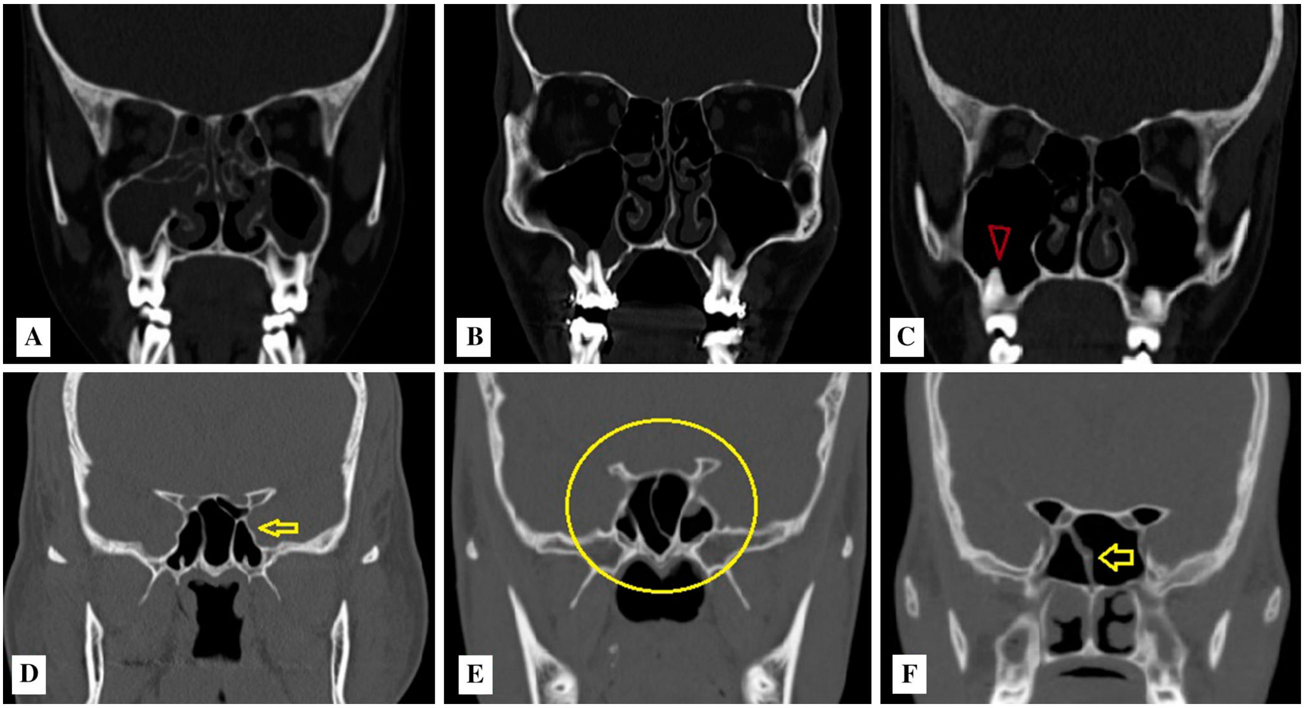

Fig. 4 Coronal images of plain computer tomography of paranasal sinus; first row showing protrusion of tooth root into the maxillary sinus, **a** with maxillary sinus opacification, **b** mucosal thickening and **C** no opacification; second row showing unsafe sphenoid septa attached, **d** to both optic nerve and carotid artery, **e** to carotid artery and **f** to optic nerve

seen in 126 patients. Pneumatization of the MT (Fig. 1a–c), ST and IT were respectively seen in 74, 6, and one patient. The presence of the HC (Fig. 1d, e) and the OC (Fig. 1f) were noted in 59 and 35 patients, respectively. Sixty-five of our patient had pneumatization of the CG (Fig. 2a), 41 each of the nasal septum (Fig. 2b) and the ACP (Fig. 2c), and 71 had that of PB (Fig. 2d–f). In our study, the most common type of sphenoid pneumatization was post-sellar type (Fig. 3d) followed by sellar type (Fig. 3c). Majority of the patients had Kero's type II olfactory fossa (Fig. 3j), and 5% of patients had low lying cribriform plate (Fig. 3k). The optic nerve's relationship to the sphenoid sinus wall was commonly representative of Delano type II (Fig. 3f).

Interestingly, the maxillary sinus had septation in 9 of our patients, all of them extending from the lateral wall to the floor. In 37 of study patients the sphenoid septation had an attachment to either of the optic nerve (Fig. 4f) or carotid artery (Fig. 4e) or both (Fig. 4d), constituting an unsafe pattern of septation. The association between the anatomical characteristics with each other were calculated by using a contingency table and Pearson Chi Square test, as shown in Table 2. However, most of the associations could not attain statistical significance as except a few. In our study, only the presence of OC was found to be significantly related to septal pneumatization ($p = 0.03$) and pneumatization of CG ($p = 0.05$). In our set of patients with chronic rhinosinusitis, radiological opacification of maxillary sinus showed significant association separately with the DNS ($p = 0.03$) and with the CB ($p = 0.04$). Statistically, the location of tooth root protruding through the maxillary floor into the sinus (Fig. 4a–c) did not have any relationship with the maxillary sinus opacification.

Discussion

This study has evaluated almost all of the clinically relevant anatomical variations that could be appreciated in the CT images of paranasal sinuses belonging to more than 150 patients. The results of our study are in line with the rates reported by different authors over the last two decades, concerning most of the variations except a few as summarized in Table 3. In fact, for many anatomical variations, the prevalence rates in the reported literature itself exhibit non-uniformity and a wide range of distribution. The primary reason for this variability across the studies could be attributed not only to the geographical, racial and ethnic differences between the study participants in different studies, but also to the differences in methodological considerations among these studies. While most studies have reported the prevalence rates for the number of included patients, some studies' reports are based on the number of sides or sinuses evaluated and not the patients involved, as shown in Table 3. To make it comparable with

Table 2 Association between various anatomical variations, and between the clinically relevant anatomical variations with corresponding radiological abnormalities

Anatomical variation or clinical abnormality (a)	Association		
	Variation (b)	(a) with (b)	p value
DNS (n = 126)	CB	63	0.58
	ST	4	0.83
	Sp	32	0.49
	HC	51	0.42
	OC	27	0.25
	PB	59	0.91
	CG	57	0.22
	ACP	34	0.91
CB (n = 74)	ST	4	0.15
	Sp	24	0.10
	HC	32	0.30
	OC	19	0.47
	PB	36	0.69
	CG	37	0.09
	ACP	22	0.48
OC (n = 35)	ST	2	0.36
	Sp	14	***0.03***
	HC	17	0.18
	PB	17	0.83
	ACP	9	0.82
	CG	20	***0.05***
Maxillary sinus opacification (n = 106 patients, 163 sides[a])	DNS	84	***0.03***
	HC	57[a]	0.54
	CB	46[a]	***0.005***
	TR	67[a]	0.36

ACP Anterior clinoid process pneumatized, *CB* Concha bullosa, *CG* Crista Galli pneumatized, *DNS* Deviated nasal septum, *HC* Haller cell, *OC* Onodi cell, *PB* Pterygoid base pneumatized, *Sp* Septum pneumatized, *ST* Superior turbinate pneumatized and *TR* Tooth root inside the sinus

[a]Represents the numbers out of 302 sides

either of these type of reports, we have reported prevalence rates of all anatomical factors separately for the number of patients and the number of sides as the denominator, except for the variations in the unpaired midline structures like nasal septum, and CG.

The anatomical variations like DNS, CB, HC, OC, pneumatization of PB, and ACP had been studied in detail by various authors with the inclusion of participants from across the globe. Our results were within the reported range in the literature for all of these factors. On the other hand, only a few studies have discussed the pneumatization status of nasal septum and CG, and the prevalence rates of these two in our study were considerably more than the several previous reports. However, studies by Mladina et al. respectively showed pneumatization in the perpendicular plate of ethmoid in 34.4% and pneumatization of CG in 66.6%, by doing cone-beam CT of human skull bones [40, 41]. Contrary to pneumatized nasal septum seen in 2% of the cases reported by Dua et al. [20] that were involving vomer bone of septum, we identified 27% our cases to have nasal septal pneumatization, and all were seen involving the perpendicular plate of the ethmoid, similar to findings of Mladina and group [40]. 43% of pneumatized CG seen in our study is between the 22.9% reported by cobzeanu et al. and the 66.6 by Mladina et al [32, 41]. The literature review of the other existing studies rates the CG pneumatization to vary between 3 and 37.5% [32, 41]. Further studies in this regard can validate the appropriate prevalence rates of these.

Presence of DNS was seen in 83% of our patients, most of whom were symptomatic in terms of nasal obstruction, independent of the type of deviation. As reported previously [46], most of the other anatomical variations were

Table 3 Comparison of anatomical variations reported by different authors over the last two decades

Authors	SS	DNS	CB	HC	OC	ST	Sp	CG	PB	ACP	MS	USS
Alrumaih [28]	121	–	55.4	39.7	28.9	–	–	–	73	–	23	–
Alsowey [29]	240	48.8	30.6	11.2	55.8[a]	–	–	–	–	–	–	–
Anusha [30]	300	–	–	–	14.3	–	–		–	–	–	36
Batra [31][b]	64	–	–	–	–	–	–	–	–	–	–	37.5[a]
Cobzeanu [32]	205	–	–	–	–	29.7	–	22.9	–	–	–	–
da Costa [33]	597	–	–	–	–	–	–	–	–	25.5	–	–
Dal Secchi [14]	90	–	–	–	–	–	–	–	–	–	–	14
Dua [20][c]	50	44	16	16	6	–	2	–	–	–	6	–
Hajiioannou [34]	99	–	–	–	–	–	–	14.1	–	–	–	–
Hewaidi [35]	300	–	–	–	–	–	–	–	29	15.3	–	–
Jones [36]	200	24	20	9	8	–	–		–	–	–	–
Kaya [11]	350	89.7	51[a]	25[a]	14	–	–	–	14[a]	21.1[a]	–	–
Kazkayasi [37]	267	–	–	–	–	–	–	–	39.7	17.2	–	–
Litu [38]	50	64	38	–	–	–	–	–	–	–	–	–
Lu [2][b]	218								22.3	5		
Mamatha [18][c]	40	65	15	17.5	–	–	–		–	–	–	–
Mazza [39]	100	–	29	5	9	–	–		–	–	–	–
Mladina [40][b]	93	–	–	–	–	–	34.4	–	–	–	–	–
Mladina [41][b]	102	–	–	–	–	–	–	66.6	–	–	–	–
Ozcan [42]	384	–	48	–	–	12.2	–		–	–	–	–
Ozturan [43]	160	–	–	–	66.2[a]	–	–	–	–	–	–	–
Rahmati [26]	103	–	–	–	–	–	–	–	38.9	33.1	–	–
Tomovic [4]	170	–	–	–	65.3	–	–	–	–	–	–	–
Unal [13]	56	–	–	–	8[a]	–	–	–	–	24.1[a]	–	26.7[a]
Wada [44]	261	–	–	–	50.8[a]	–	–	–	–	–	–	–
Yazici [45]	120	36.6	44.2	20.8	30.8	30.8	–	–	18.3	29.2	–	–
Our study[c]	151	83.4	49	39	23.1	3.9	27.1	43	47	27.1	5.9	24
			35.4[a]	33.4[a]	19.5[a]	2.3[a]			22.1[a]	36.4[a]	3.3[a]	15.2[a]

All numbers are in percentages

ACP Anterior clinoid process pneumatized, *CB* Concha bullosa, *CG* Crista Galli pneumatized, *DNS* Deviated nasal septum, *HC* Haller cell, *MS* Maxillary septa, *OC* Onodi cell, *PB* Pterygoid base pneumatized, *Sp* Septum pneumatized, *SS* Sample size, *ST* Superior turbinate pneumatized and *USS* Unsafe sphenoid septa

[a]Represents the percentages considering each side separately in the denominator, whereas the rest of the percentages are for the number of patients

[b]Studies that have analyzed the radiology of human skull bone

[c]Studies from India

found to be higher in patients with DNS, however, we could not find any statistically significant association between them. With respect to CB, though the frequent type in our study was 'extensive type' like in other studies, we had more of unilateral CB than what is reported in the literature [42, 46, 47]. Statistically, the presence of CB had no bearing on the pneumatization of any other ethmoidal or sphenoidal bony landmark in paranasal sinuses of our study cohort. Some authors have shown a significant correlation between the surface area of CB and the number of aerated ethmoid structures [48]; however, such an analysis was beyond the scope of our objective and methodology. Nevertheless, in our study the presence of OC showed significant association with the aeration of septal part of the perpendicular plate of the ethmoid, but not with that of other ethmoidal or sphenoidal bony parts like ST and CG or PB and ACP, respectively. In practical, the pneumatization status of PB and ACP are very relevant both prognostically as well as therapeutically. The PB is related to and can expose the maxillary nerve and the vidian nerve into the sphenoid or posterior ethmoid sinus. Similarly, the ACP pneumatization can play a role in protrusion or dehiscence of the optic nerve and less commonly the internal carotid artery into the sphenoid sinus [17, 35, 37, 49, 50], making them vulnerable to the disease process or the surgical trauma. Therapeutically, the aeration pattern of PB can be utilized as a sinonasal corridor to control lesions of middle and posterior skull base through endoscopic endonasal transpterygoid [16], intrasphenoidal or transsphenoidal approaches [17]. As discussed earlier, the pneumatization rates of PB and ACP in our study were very much comparable to those in the literature. But what needs to be critically appreciated here is the rate of asymmetry of these anatomical structures between the two sides in the same patient. The asymmetry across the various anatomical characteristics can vary from 10 to 50% [26, 36, 42, 47], as was the case in our study also.

Another important anatomical consideration that is crucial for pre-operative planning of surgical approaches to structures or lesions surrounding the sphenoid like the pituitary gland, cavernous sinus, vidian nerve and maxillary nerve, is the pneumatization pattern of sphenoid sinus itself [3, 16, 17, 27, 35]. Post-sellar type of pneumatization being the most prevalent type like in our study as well as in other studies [3, 7, 26, 31] or second common type [15, 24, 25, 27] following sellar, provides a wide surgical window through sphenoid or pterygoid base during skull base surgery. However, attention has to be given to some of the other anatomical perturbations in the sphenoid sinus that could also be detrimental in preventing surgical morbidity. In our study, septation of sphenoid was found to be unsafe in 24% of the patients, most of which were having an attachment to the carotid canal, some to the optic canal and a few to both the optic and carotid canal. Attachment of sphenoid septation to the carotid canal has been reported by others in up to 37.5% of the cases [13–15, 31]. In 2 of our cases, the carotid artery was dehiscent inside the sphenoid sinus, and optic nerve was coursing through the sphenoid sinus (Type III Delano) in 22.5% of our patients. The reported rate of 'protrusion or bony dehiscence of internal carotid artery' into the sphenoid sinus is as high as 37. 5% and that of 'protruding or dehiscent optic nerve' is up to 30% [13, 21, 23, 24, 28, 30, 35, 37, 43, 45, 49]. Knowledge about these variations in sphenoid sinus anatomy including the pneumatization pattern, the attachment of inter-sinus septa and the vulnerable neurovascular anatomy is of utmost importance to ensure surgical safety. When it comes to prevention of surgical morbidity, the depth of olfactory fossa is another critical area which needs to be assessed in the pre-operative setting to prevent any inadvertent damage to the anterior skull base and resultant cerebrospinal fluid leak. As seen in our cases and in the literature, though majority would have a favorable 'Kero's type II olfactory fossa' [28], the low lying 'Kero's type III olfactory fossa' is not uncommon and needs a careful planning as well as meticulous handing of skull base while performing sinus or skull base surgeries.

Finally, we hypothesized the possible involvement of tooth root protrusion into the maxillary sinus in the causation of maxillary sinus opacification, independent of other anatomical variations like DNS, CB, and HC. However, on analysing our data, only the DNS and the CB showed significant association with radiologically opacified maxillary sinuses; but the tooth root protrusion and HC did not. Though the location of tooth root especially had no bearing on maxillary sinus opacification in this study, we could not incorporate the status of the tooth as healthy or as caries, in the analysis. It is still possible that the chronically diseased tooth having its root protruding into the sinus may have some implication in causing maxillary sinusitis. On the other hand, though we identified maxillary septa in 6% of cases, the rate that is variable in literature [20, 51], and the implication of maxillary sinus septa in pathophysiology of maxillary sinusitis is yet to be determined. Further studies are needed to understand these associations. Our study, though unique in many ways has some limitations. Being retrospective in nature, no comparison or association of anatomical variations with the endoscopic findings could be incorporated in our study, and similarly, we could not analyse the surgical results, nor could we correlate them with the anatomical variations.

Conclusions

Almost all of the anatomical variations noted in this study had the prevalence rates that were comparable with the literature. DNS, CB are the two significant anatomical variations that were encountered, and both were found to have an association with maxillary sinus opacification in chronic rhinosinusitis patients. The associations between most of the anatomical changes were not significant statistically. Similar to previous reports in the literature, the asymmetry between the sides in the same patient is quite commonly seen in our study. Overall, considering the gross variability in the critical neurovascular and bony anatomy of paranasal sinuses, it is imperative that these variations be studied thoroughly before any interventions involving the sinuses.

Compliance with Ethical Standards

Conflict of interest All authors declare that they have no conflict of interest.

References

1. Tan HKK, Ong YK (2007) Sphenoid sinus: an anatomic and endoscopic study in Asian cadavers. Clin Anat N Y N 20:745–750
2. Lu Y, Pan J, Qi S, Shi J, Zhang X, Wu K (2011) Pneumatization of the sphenoid sinus in Chinese: the differences from Caucasian and its application in the extended transsphenoidal approach. J Anat 219:132–142
3. Özer CM, Atalar K, Öz II, Toprak S, Barut Ç (2018) Sphenoid sinus in relation to age, gender, and cephalometric indices. J Craniofac Surg 29:2319–2326
4. Tomovic S, Esmaeili A, Chan NJ, Choudhry OJ, Shukla PA, Liu JK et al (2012) High-resolution computed tomography analysis of the prevalence of Onodi cells. The Laryngoscope 122:1470–1473
5. Muñoz-Leija MA, Yamamoto-Ramos M, Barrera-Flores FJ, Treviño-González JL, Quiroga-Garza A, Méndez-Sáenz MA et al (2018) Anatomical variations of the ethmoidal roof: differences between men and women. Eur Arch Oto-Rhino-Laryngol 275:1831–1836
6. Badia L, Lund VJ, Wei W, Ho WK (2005) Ethnic variation in sinonasal anatomy on CT-scanning. Rhinology 43:210–214
7. Hiremath SB, Gautam AA, Sheeja K, Benjamin G (2018) Assessment of variations in sphenoid sinus pneumatization in Indian population: a multidetector computed tomography study. Indian J Radiol Imaging 28:273–279
8. Burulday V, Muluk NB, Akgül MH, Kaya A, Öğden M (2016) Presence and types of anterior clinoid process pneumatization, evaluated by Multidetector Computerized Tomography. Clin Invest Med 39:E105–E110
9. Karki S, Pokharel M, Suwal S, Poudel R (2016) Prevalence of anatomical variations of the sinonasal region and their relationship with chronic rhinosinusitis. Kathmandu Univ Med J KUMJ 14:342–346
10. Johari HH, Mohamad I, Sachlin IS, Aziz ME, Mey TY, Ramli RR (2018) A computed tomographic analysis of frontal recess cells in association with the development of frontal sinusitis. Auris Nasus Larynx 45:1183–1190
11. Kaya M, Çankal F, Gumusok M, Apaydin N, Tekdemir I (2017) Role of anatomic variations of paranasal sinuses on the prevalence of sinusitis: computed tomography findings of 350 patients. Niger J Clin Pract 20:1481–1488
12. Socher JA, Santos PG, Correa VC, e Silva LCDB (2013) Endoscopic surgery in the treatment of crista galli pneumatization evolving with localizated frontal headaches. Int Arch Otorhinolaryngol 17:246–250
13. Unal B, Bademci G, Bilgili YK, Batay F, Avci E (2006) Risky anatomic variations of sphenoid sinus for surgery. Surg Radiol Anat SRA 28:195–201
14. Dal Secchi MM, Dolci RLL, Teixeira R, Lazarini PR (2018) An analysis of anatomic variations of the sphenoid sinus and its relationship to the internal carotid artery. Int Arch Otorhinolaryngol 22:161–166
15. Hamid O, El Fiky L, Hassan O, Kotb A, El Fiky S (2008) Anatomic variations of the sphenoid sinus and their impact on trans-sphenoid pituitary surgery. Skull Base Off J North Am Skull Base Soc Al 18:9–15
16. Kasemsiri P, Solares CA, Carrau RL, Prosser JD, Prevedello DM, Otto BA et al (2013) Endoscopic endonasal transpterygoid approaches: anatomical landmarks for planning the surgical corridor. The Laryngoscope 123:811–815
17. Lee J-C, Kao C-H, Hsu C-H, Lin Y-S (2011) Endoscopic transsphenoidal vidian neurectomy. Eur Arch Oto-Rhino-Laryngol Off J Eur Fed Oto-Rhino-Laryngol Soc EUFOS Affil Ger Soc Oto-Rhino-Laryngol Head Neck Surg 268:851–856
18. Mamatha H, Shamasundar NM, Bharathi MB, Prasanna LC (2010) Variations of ostiomeatal complex and its applied anatomy: A CT scan study. Indian J Sci Technol 3:904–907
19. Vidya CS, Raichurkar K (2015) Anatomic variation of sphenoid sinus in mysore based population: ct scan study. Int J Anat Res 3:1611–1614
20. Dua K, Chopra H, Khurana AS, Munjal M (2005) CT scan variations in chronic sinusitis. Indian J Radiol Imaging. 15:315
21. Itagi RM, Adiga CP, Kalenahalli K, Goolahally L, Gyanchandani M (2017) Optic nerve canal relation to posterior paranasal sinuses in indian ethnics: review and objective classification. J Clin Diagn Res JCDR 11:TC01–TC03
22. Keros P (1962) On the practical value of differences in the level of the lamina cribrosa of the ethmoid. Z Laryngol Rhinol Otol. 41:809–813
23. DeLano MC, Fun FY, Zinreich SJ (1996) Relationship of the optic nerve to the posterior paranasal sinuses: a CT anatomic study. AJNR Am J Neuroradiol 17:669–675
24. Tomovic S, Esmaeili A, Chan NJ, Shukla PA, Choudhry OJ, Liu JK et al (2013) High-resolution computed tomography analysis of variations of the sphenoid sinus. J Neurol Surg B Skull Base 74:82–90
25. Sengul G, Ertürk M, Varol T (2005) Variations in sphenoid sinus anatomy with special emphasis on pneumatization and endoscopic anatomic distances. Neurosci Riyadh Saudi Arab 10:79–84
26. Rahmati A, Ghafari R, AnjomShoa M (2016) Normal variations of sphenoid sinus and the adjacent structures detected in cone beam computed tomography. J Dent Shiraz Iran 17:32–37
27. Štoković N, Trkulja V, Dumić-Čule I, Čuković-Bagić I, Lauc T, Vukičević S et al (2016) Sphenoid sinus types, dimensions and relationship with surrounding structures. Ann Anat 203:69–76
28. Alrumaih RA, Ashoor MM, Obidan AA, Al-Khater KM, Al-Jubran SA (2016) Radiological sinonasal anatomy exploring the Saudi population. Saudi Med J 37(5):521–526
29. Alsowey AM, Abdulmonaem G, Elsammak A, Fouad Y (2017) Diagnostic performance of multidetector computed tomography [MDCT] in diagnosis of sinus variations. Pol J Radiol 82:713–725
30. Anusha B, Baharudin A, Philip R, Harvinder S, Shaffie BM, Ramiza RR (2015) Anatomical variants of surgically important landmarks in the sphenoid sinus: a radiologic study in Southeast Asian patients. Surg Radiol Anat 37:1183–1190
31. Batra PS, Citardi MJ, Gallivan RP, Roh H-J, Lanza DC (2004) Software-enabled computed tomography analysis of the carotid artery and sphenoid sinus pneumatization patterns. Am J Rhinol 18:203–208
32. Cobzeanu MD, Bâldea V, Bâldea MC, Vonica PS, Cobzeanu BM (2014) The anatomo-radiological study of unusual extrasinusal pneumatizations: superior and supreme turbinate, crista galli process, uncinate process. Romanian J Morphol Embryol 55(3 Suppl):1099–1104
33. da Costa MDS, de Oliveira Santos BF, de Araujo Paz D, Rodrigues TP, Abdala N, Centeno RS et al (2016) Anatomical variations of the anterior clinoid process: a study of 597 skull base computerized tomography scans. Oper Neurosurg 12:289–297
34. Hajiioannou J, Owens D, Whittet HB (2010) Evaluation of anatomical variation of the crista galli using computed tomography. Clin Anat 23:370–373
35. Hewaidi G, Omami G (2008) Anatomic variation of sphenoid sinus and related structures in Libyan population: CT scan study. Libyan J Med 3:128–133
36. Jones NS, Strobl A, Holland I (1997) A study of the CT findings in 100 patients with rhinosinusitis and 100 controls. Clin Otolaryngol Allied Sci 22:47–51

37. Kazkayasi M, Karadeniz Y, Arikan OK (2005) Anatomic variations of the sphenoid sinus on computed tomography. Rhinology 43:109–114
38. Litu MA, Bhuiyan MR, Mahmud S, Masud MK, Khan MA, Rahman MA et al (2016) Structural variations of nose and paranasal sinuses in various sinonasal pathologies: tomographic study of 50 cases in Bangladeshi people. Mymensingh Med J 25:686–690
39. Mazza D, Bontempi E, Guerrisi A, Del Monte S, Cipolla G, Perrone A et al (2007) Paranasal sinuses anatomic variants: 64-slice CT evaluation. Minerva Stomatol 56:311–318
40. Mladina R, Antunović R, Cingi C, Bayar Muluk N, Skitarelić N (2017) Sinus septi nasi: anatomical study. Clin Anat 30:312–317
41. Mladina R, Antunović R, Cingi C, Muluk NB, Skitarelić N, Malić M (2017) An anatomical study of pneumatized crista galli. Neurosurg Rev 40:671–678
42. Ozcan KM, Selcuk A, Ozcan I, Akdogan O, Dere H (2008) Anatomical variations of nasal turbinates. J Craniofac Surg 19:1678–1682
43. Ozturan O, Yenigun A, Degirmenci N, Aksoy F, Veyseller B (2013) Co-existence of the Onodi cell with the variation of perisphenoidal structures. Eur Arch Oto-Rhino-Laryngol 270:2057–2063
44. Wada K, Moriyama H, Edamatsu H, Hama T, Arai C, Kojima H et al (2015) Identification of Onodi cell and new classification of sphenoid sinus for endoscopic sinus surgery. Int Forum Allergy Rhinol 5:1068–1076
45. Yazici D (2019) The effect of frontal sinus pneumatization on anatomic variants of paranasal sinuses. Eur Arch Oto-Rhino-Laryngol 276:1049–1056
46. Koo SK, Kim JD, Moon JS, Jung SH, Lee SH (2017) The incidence of concha bullosa, unusual anatomic variation and its relationship to nasal septal deviation: a retrospective radiologic study. Auris Nasus Larynx 44:561–570
47. İla K, Yilmaz N, Öner S, Başaran E, Öner Z (2018) Evaluation of superior concha bullosa by computed tomography. Surg Radiol Anat SRA 40:841–846
48. Odat H, Al-Qudah M (2016) Concha bullosa and ethmoid structures pneumatization: the effect of altitude and other variables. J Craniofac Surg 27:e667–e669
49. Rereddy SK, Johnson DM, Wise SK (2014) Markers of increased aeration in the paranasal sinuses and along the skull base: association between anatomic variants. Am J Rhinol Allergy 28:477–482
50. Mohebbi A, Rajaeih S, Safdarian M, Omidian P (2017) The sphenoid sinus, foramen rotundum and vidian canal: a radiological study of anatomical relationships. Braz J Otorhinolaryngol 83:381–387
51. Lozano-Carrascal N, Salomó-Coll O, Gehrke SA, Calvo-Guirado JL, Hernández-Alfaro F, Gargallo-Albiol J (2017) Radiological evaluation of maxillary sinus anatomy: A cross-sectional study of 300 patients. Ann Anat 214:1–8